Magnetic properties of β-phase iron-germanium

P. J. Schurer,* N. J. G. Hall, and A. H. Morrish
Department of Physics, University of Manitoba, Winnipeg, Manitoba, R3T 2N2
(Received 28 December 1977; revised manuscript received 25 April 1978)

The results of x-ray diffraction, magnetization, and Mössbauer measurements on β-phase iron-germanium alloys are presented. It is found that iron atoms are present at all three $2(a)$, $2(d)$, and $2(c)$ sites. The different hyperfine fields at these sites appear to be determined primarily by different iron magnetic moments. Values of $\mu_a = 1.3\mu_B$, $\mu_d = 1.9\mu_B$, and $\mu_c = 2.4\mu_B$ are proposed for the iron atoms at $2(a)$, $2(d)$, and $2(c)$ sites, respectively. Different anisotropic contributions D_{an} to the hyperfine field are found for the three lattice positions; D_{an} is largest for the $2(c)$ sites. The magnetic-anisotropy constant K_1 is also largest for the $2(c)$ sites. The power dependence of the anisotropy constant K_1 on the magnetization is close to cubic.

I. INTRODUCTION

The β phase of the iron-germanium system has been the subject of investigation and controversy during the last 20 years, especially with regard to its magnetic properties. There is a large number of conflicting experimental results and in turn interpretations differ widely. A review of the results obtained previously is given in this section; several of them will be considered again later in comparison with the results obtained in this study.

The phase diagram now generally accepted for the β-phase region was reported by Kanematsu and Ohoyama.[1] The material crystallizes in the $B8_2$ hexagonal structure[2-5] although a small distortion may be present.[6] There are three different sites, the unit cell containing two of each. The positions are $2(a)$ at 000 and $00\frac{1}{2}$, $2(d)$ at $\frac{1}{3}\frac{2}{3}\frac{3}{4}$ and $\frac{2}{3}\frac{1}{3}\frac{1}{4}$, and $2(c)$ at $\frac{1}{3}\frac{2}{3}\frac{1}{4}$ and $\frac{2}{3}\frac{1}{3}\frac{3}{4}$. From x-ray diffraction and picnometric density measurements Kanematsu and Ohoyama[7,8] propose essentially that the unit-cell formula is $Fe_{2+2x}Ge_2V_{2-2x}$ $(\frac{1}{2}<x<1)$, with two Ge atoms at the 2(c) sites, two Fe atoms at the 2(a) sites, and $2x$ Fe atoms and $2-2x$ vacancies (denoted by V) at the $2(d)$ sites. This distribution of atoms has recently been called into doubt by Daniels *et al.*[9] who, unable to fit their Mössbauer spectra with two six-line absorption patterns, propose that the $2(a)$ sites are filled with iron and the remaining iron and germanium atoms are distributed on both the $2(d)$ and $2(c)$ sites leaving vacancies on both.

The magnetic moments assigned to the iron atoms by different authors vary widely (Table I). Consequently several magnetic structures involving different canting angles θ, up to 90°, have been suggested. However, Hall *et al.*[10] have indicated recently that the results of a Mössbauer study of single-crystal $Fe_{1.67}Ge$ are in agreement with a collinear spin structure. The canting of the iron magnetic moments is zero, or at most small.

Magnetization measurements have established that the c axis is the hard magnetization direction but there are conflicting reports about the anisotropy in the basal plane.[10-13]

Most Mössbauer-effect measurements have been performed at one[11,14-17] or two[9] temperatures. Bhargava and Iyengar[18] have studied $Fe_{1.67}Ge$ at temperatures between 77 K and up to above the Curie temperature T_F.

The Mössbauer spectra are complex due to the presence of several overlapping absorption patterns which are poorly resolved. Several interpretations of the spectra have been presented. Fatseas *et al.*[17,19] have fitted the spectra assuming that the iron atoms are present only at $2(a)$ and $2(d)$ sites and that the absorption patterns corresponding to these two sites consist of several components which are attributed to different vacancy distributions in neighboring shells. In another interpretation,[9,18] the iron atoms are present at all three lattice sites and the spectra are fitted using three components. Three well-resolved components are observed in a Mössbauer spectrum

TABLE I. Magnetic moments (in units of μ_B) and canting angles attributed by different authors to iron atoms at $2(a)$, $2(d)$, and $2(c)$ sites in the unit cell of β-phase iron-germanium.

Reference	μ_a	θ_a	μ_d	θ_d	μ_c	θ_c
5	1.3(1)		1.1(1)	28°		
6	1.4(1)		1.9(1)			
7	2	~90°	3			
9	2		4	0°–22°	4	90°
11	1.6(2)		0.5(2)			

taken with external fields up to 50 kOe parallel to the c axis of single crystal $Fe_{1.67}Ge$.[10] The question arises now whether the three components correspond to iron atoms at three different lattice sites or can be explained by the vacancy distribution. In order to investigate this point further it was decided to study two more single-crystal samples with iron concentrations different from $Fe_{1.67}Ge$, namely, $Fe_{1.80}Ge$ and $Fe_{1.55}Ge$. In addition two polycrystalline samples enriched in Fe^{57} with composition $Fe_{1.95}Ge$ and $Fe_{1.70}Ge$ were prepared for a temperature-dependent Mössbauer study and for an investigation of the effects of different heat treatments.

In view of the controversies described above, it was considered important in the analysis of the experimental results to combine the Mössbauer data with those of x-ray diffraction and magnetization measurements performed on the same sample.

II. SAMPLE PREPARATION AND EXPERIMENTAL PROCEDURE

To prepare polycrystalline samples, stoichiometric amounts of germanium powder (99.999% pure) and iron sponge (99.999% pure) were mixed thoroughly and pressed into a pellet. The iron had been reduced previously by heating at 700 °C while maintaining a flow of hydrogen gas. The pellet was sealed off in a Vycor tube filled with $\simeq 100$ Torr of argon. Two 100-mg samples of $Fe_{1.95}Ge$ and $Fe_{1.70}Ge$ both 20% enriched in Fe^{57} have been prepared. The $Fe_{1.70}Ge$ sample was maintained at 1070 °C for 24 h and quenched. The effects of several heat treatments were investigated for the $Fe_{1.95}Ge$ sample. As will be discussed later, pure β phase was obtained by quenching as fast as possible from 1100 °C.

The samples were investigated by powder-diffractometer measurements. From the line positions, values of the lattice parameters were obtained. The lattice parameters were in reasonable agreement with published data and are shown in Table II. In addition no extra lines were observed, indicating that the samples were pure β phase.

Unfortunately, α-iron has its main diffraction maxima close to the maxima of β-phase Fe-Ge, consequently x-ray diffraction is not very sensitive to small impurities of α-iron. However the hyperfine fields are quite different and Mössbauer spectra can give reliable estimates of the amount of iron impurity. Furthermore a two-phase mixture, in which the components have different Curie temperatures, may be shown to be a mixture by measuring between the two Curie temperatures, provided both impurities contain iron. These techniques were used to indicate impurities before the samples were considered acceptable.

TABLE II. Lattice parameters in angstroms of polycrystalline (20% enriched in ^{57}Fe) samples and single-crystal samples in the β-phase region of the Fe-Ge diagram.

		a	b
Polycrystalline	$Fe_{1.95}Ge$	4.044	5.027
	$Fe_{1.70}Ge$	4.022	5.025
Single-crystal	$Fe_{1.80}Ge$	4.040	5.028
	$Fe_{1.67}Ge$	4.008	5.009
	$Fe_{1.55}Ge$	3.988	5.005

A comparison of room-temperature spectra before and after the Curie-temperature measurements showed that a slight narrowing of the lines had occurred. Since this narrowing helped analysis of the complex spectra below T_F all samples were given a heat treatment at 250 °C for a few hours before further measurements were made. The origin of the line narrowing is, however, unclear.

In the literature there is some variation in the heat treatments used. Some investigators carried out an initial heat treatment to ensure homogeneity. Adelson and Austin,[5] for example, maintained their samples above the melting point for two days, whereas Yamamoto[14] sintered at 1000 °C for two days. Fatseas *et al.*[17] and Daniels *et al.*,[9] on the other hand, carried out no initial heat treatment. Recently, Eliezer *et al.*[20] performed Mössbauer measurements on mixtures of iron and germanium corresponding to $Fe_{1.7}Ge$, which had been sintered for times ranging from 10 min to 2 h at 600 °C. It can be seen from their results that after two hours the reaction is 99% complete. It appears that the initial heat treatment is unnecessary and it is the final heat treatment that determines the properties of the sample.

From the phase diagram, it can be seen that $Fe_{1.95}Ge$ alloys must be quenched from 1100 °C in order to preserve pure β phase. For lower iron content, the samples may be cooled slowly. In the literature the final heat treatments chosen are consistent with this, except that Daniels *et al.*[9] prepared all samples by cooling slowly from the melting point of iron. There have been reports that for $Fe_{1.95}Ge$ there is an unavoidable precipitate of α-iron when the alloy is quenched from 1100 °C.[8,16]

The present investigation shows that the crystalline form of $Fe_{1.95}Ge$ at room temperature depends critically on the rate of cooling from the

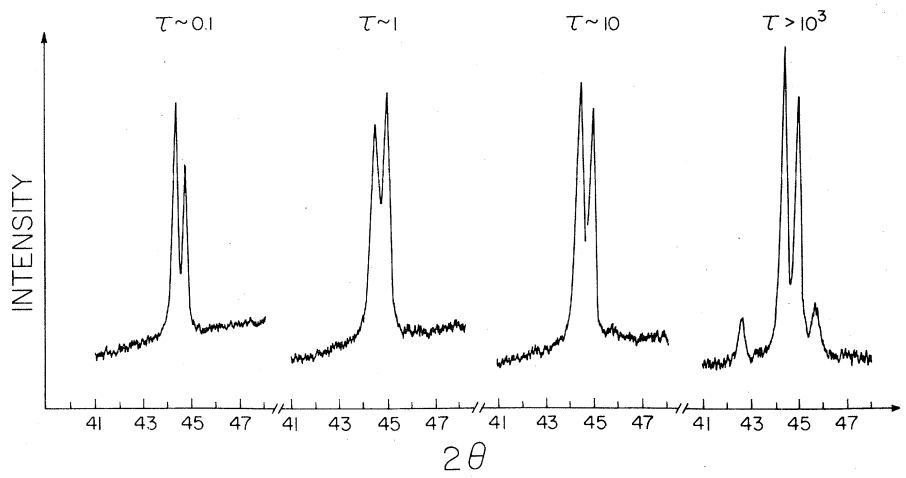

FIG. 1. Diffraction patterns of $Fe_{1.95}Ge$ for various quench rates τ.

temperature at which it is stable (1100 °C). The cooling rate can be characterized by the time τ, which is the time taken for the difference between the original temperature and room temperature to reduce by one-half. The values of τ are only approximate and are based upon observation of the time taken for the sample to stop glowing. In each case the resulting material was investigated using both x-ray diffraction and Mössbauer effect.

Powder x-ray diffractometer results for angles from 41° to 48° are shown in Fig. 1. For $\tau > 10^3$-sec impurity lines coming from hexagonal ϵ-phase Fe_3Ge are clearly observable as would be expected from the phase diagram. For $\tau \simeq 1$ sec there is apparently only β phase present as no additional lines are observed but a slight broadening can be seen. $\tau \simeq 0.1$ sec gave apparently a single phase with line shapes comparable with those obtained from $Fe_{1.70}Ge$.

The Mössbauer spectra for the same samples are shown in Fig. 2 and they show the origin of the impurity lines and the line broadening in the x-ray measurements. For $\tau > 10^3$ sec a six-line component spectrum with a hyperfine field of 240 kOe is observable which is equal to the hyperfine field measured for a sample known to be ϵ-phase Fe_3Ge.

For $\tau \simeq 10$ sec the ϵ-phase component is still present but now there is another six-line component with a hyperfine field of 330 kOe. This corresponds to bcc α-iron. The precipitate of α-iron for intermediate cooling rates observed in these Mössbauer spectra is in agreement with the results of Kanematsu[8] who observed a similar precipitate using magnetization measurements above the β-phase Curie temperature. The three-phase system is metastable and is formed only because the iron precipitate has not had time to react fully with the β phase to form ϵ phase according to the reaction:

$$2.05\,Fe + Fe_{1.95}Ge \rightarrow Fe_3Ge\,,$$

whereas for slower cooling rates no iron was observed because the reaction was complete.

On increasing the cooling rate still further until

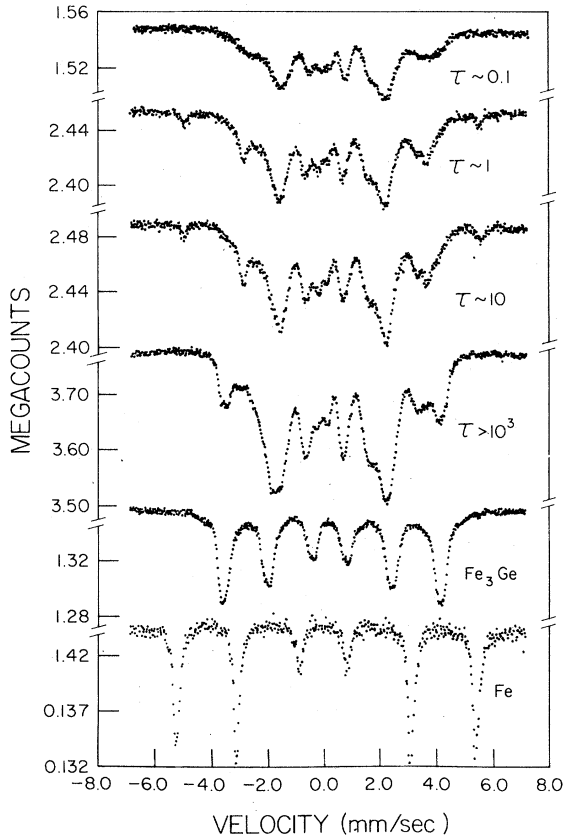

FIG. 2. Mössbauer spectra of $Fe_{1.95}Ge$ for various quench rates τ.

$\tau \simeq 1$ sec, the ϵ-phase component disappears leaving only the α-iron remaining. Now the quench is so fast that none of the precipitated iron has reacted to form the ϵ phase.

Finally by increasing the quench speed as much as possible so that $\tau \simeq 0.1$ sec a spectrum was obtained in which there was no α-iron component and this material was taken to be the pure β phase.

Single crystals were prepared by slowly cooling (10 K/h) stoichiometric mixtures of iron and germanium from 1250 °C in a quartz tube which was located inside another quartz tube. The $Fe_{1.80}Ge$ sample was removed from the furnace at 1000 °C in order to avoid a mixing of two phases. The $Fe_{1.55}Ge$ and $Fe_{1.67}Ge$ samples were allowed to cool down to 650 °C and then removed. As a final heat treatment the samples were annealed at 250 °C for at least 8 h. The results were investigated with von Laue photographs. X-ray diffraction and Mössbauer-effect measurements above T_F were used to determine the purity of the sample. No impurity phase could be detected.

Part of each single crystal was powdered and used for the preparation of three different Mössbauer absorbers. The thickness of the absorbers was ~0.3 ($mg^{57}Fe$)/cm^2. The large anisotropy permits single-crystal particles to be aligned and then immobilized in epoxy for use as disk-shaped absorbers in Mössbauer spectroscopy. In one absorber called A, the c axis lies in the plane of the absorber, whereas in a second absorber, called B, the c axis is perpendicular to this plane. Also, an absorber, called C, with randomly oriented particles was made.

Since magnetization curves (Fig. 3) for aligned single-crystal powder and a spherical sample are not significantly different, the alignment of the absorber particles can be complete. X-ray diffractograms (Fig. 4) of absorber A show only (11.0) and (30.0) reflection lines. For absorber B only (00.2) and (00.4) reflections are observed. This result confirms that excellent alignment is achieved.

The Mössbauer measurements have been performed with an Elscint constant-acceleration spectrometer which produces linewidths of 0.28 mm/sec for the outer lines of an iron calibration absorber 10-μm thick. The differential linearity of the spectrometer, as defined by Cranshaw,[21] is 0.2%. The measurements above room temperature were performed in a furnace with a temperature stability of ~0.3 K/(24 h). Those below room temperature were obtained in a cryostat manufactured by Oxford Instruments with a stability of 0.1 K/(24 h). External magnetic fields H_{ext} were produced by a Westinghouse superconducting magnet which has a negligible field decay during the time of measurement. Magnetic shielding was used to reduce stray fields to below 100 Oe at the source,

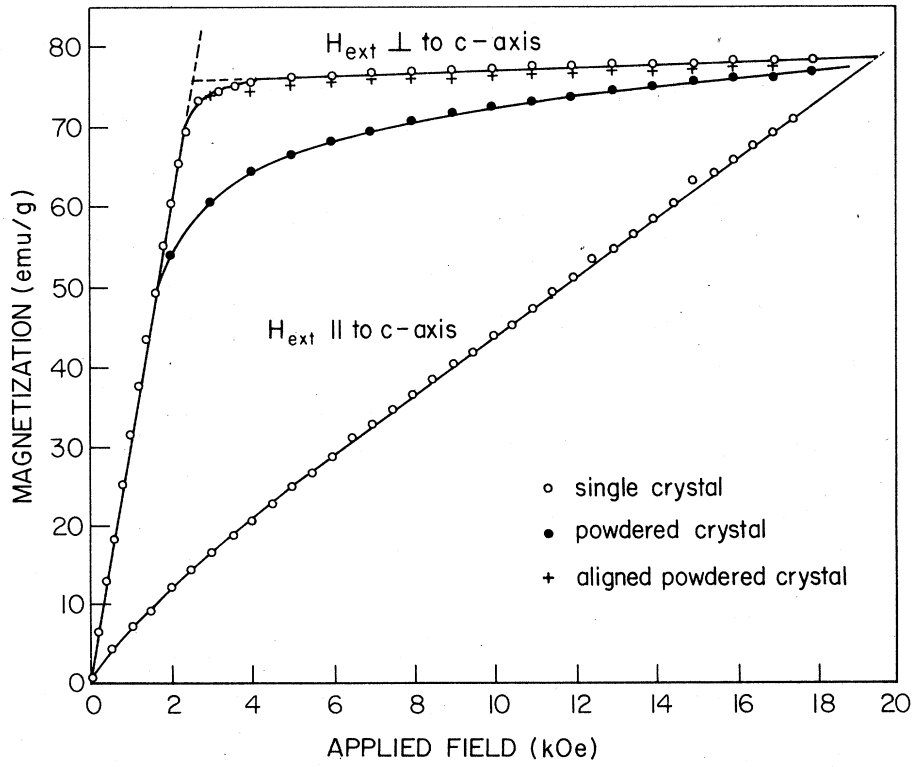

FIG. 3. Magnetization measurements on $Fe_{1.67}Ge$ at room temperature.

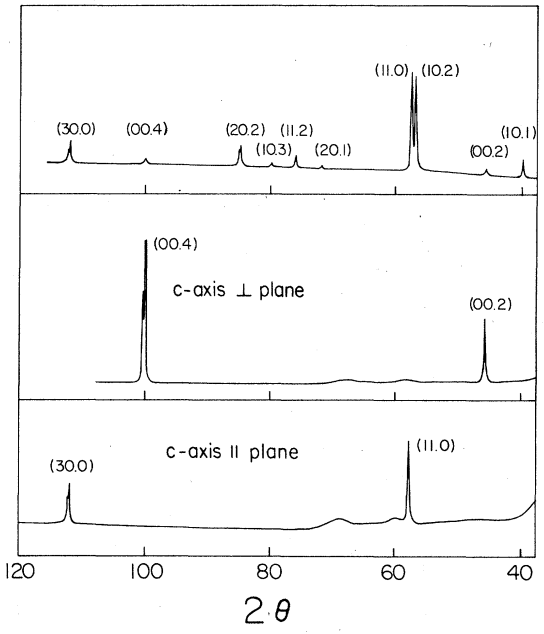

FIG. 4. X-ray diffraction patterns of $Fe_{1.67}Ge$ for random oriented single-crystal particles (top) and particles with their c axis oriented parallel or perpendicular to the plane of the x-ray target. The diffractograms were obtained using Fe $K\alpha$ radiation.

which is at room temperature during the measurements.

X-ray diffractograms were obtained using Fe $K\alpha$ radiation. The intensities of the reflection lines in the powder diffractograms have been measured accurately using a step-scanning diffractometer. Since the large magnetic anisotropy can lead to a partial alignment of the single-crystal particles in the x-ray target, the particles were mixed with benzophenon powder in order to keep the particle orientation random.

For the magnetization measurements a small piece of each of the three samples was ground until it was close to spherical. The measurements were made with a vibrating sample magnetometer in fields up to 18 kOe and temperatures between 4.2 K and the Curie temperatures T_F. The magnetometer was calibrated with a nickel sample obtained from Johnson-Mathey Chemicals Ltd. For such a sample absolute values of the magnetization have been reported by Crangle and Goodman.[22] First, each sample was investigated with the c axis oriented perpendicular to the applied field H_{ext}. Then the magnetization in the basal plane can be determined. Second, each sample was aligned such that H_{ext} is parallel to a plane which contains an easy direction and the c axis. Then the magnetization in the easy direction as well as in the hard direction can be studied. The saturation magnetization in the easy direction was the same for all three samples for both geometrical arrangements.

III. EXPERIMENTAL RESULTS

A. Magnetization measurements

Saturation of the magnetization along the easy direction occurred for $H_{app} \simeq 4$ kOe, and along the hard axis for $H_{app} \simeq 25$ kOe (Fig. 3). The values of the magnetization, $\sigma_{0,0}$, at 0 K extrapolated to zero internal field are shown in Table III. Up till now measurements below 77 K have not been reported. Consequently the values of $\sigma_{0,0}$ found in the literature must be extrapolations. A value of $\sigma_{0,0} = 89$ emu/g was reported by Tawara[12] for single crystal $Fe_{1.67}Ge$. Unfortunately the composition of the single crystal used by Katsuraki[11] is uncertain. Therefore the results of that study will not be used for comparison here. Other saturation magnetization values found in the literature were determined by using powder samples perhaps consisting of single-crystal particles.[5,7] As a consequence of the large magnetic anisotropy it is necessary to have each particle in these samples properly aligned.

The $\sigma_{0,0}$ values published by Kanematsu and Ohoyama[7] are in general lower than our values, in particular for the $Fe_{1.55}Ge$ sample. Also the value reported by Adelson and Austin[5] for $Fe_{1.60}Ge$ is lower than our value. Samples with incompletely aligned particles may possibly be the source of this discrepancy. As an example, Fig. 3 shows that the magnetization of a nonaligned single-crystal powder is 10% lower at 9 kOe than that of the spherical sample. On the other hand, the same figure shows that the magnetization of a fully aligned single-crystal powder sample has the same value as that of the sphere.

The basal plane was found to be an easy magnetization plane in which no threefold anisotropy could be detected. This finding is consistent with the magnetic torque measurements of Katsuraki.[11] However, Becker and Symes[13] reported that the basal anisotropy must be greater than 1.5×10^4 erg/cm^3 on the basis of x-ray measurements on a magnetically aligned sample of $Fe_{1.72}Ge$ single-

TABLE III. Saturation magnetization values $\sigma_{0,0}$ in emu/g and in Bohr magnetons per formula unit.

	emu/g	μ_B/(formula unit)
$Fe_{1.80}Ge$	95.1(4)	2.95
$Fe_{1.67}Ge$	89.9(4)	2.67
$Fe_{1.55}Ge$	84.3(3)	2.40

crystal particles. They decided that the a axis was the easy direction in the basal plane.

In an effort to reproduce these results we have performed an x-ray diffraction study on the Mössbauer absorbers A, B, and C. As discussed in Sec. II in absorber A the c axis lies in the plane, whereas in absorber B the c axis is perpendicular to the plane. In absorber C the particles are oriented randomly.

X-ray diffraction will only show reflections from sets of planes whose normals are perpendicular to the plane of the sample. The results are shown in Fig. 4. The presence of the epoxy produces the broad background lines in samples A and B. For sample A only the (11.0) and (30.0) lines were observed. Since the normal to the (30.0) set of planes is not an a-axis direction we conclude that, at least for the particles in our samples, the a axes are not all aligned perpendicular to the plane of the sample. This result therefore does not confirm the interpretation of Becker and Symes[13] who have reported the presence of the (11.0) line only.

The measurement of the magnetization along the hard direction with $\vec{H}_{ext} \| \vec{c}$ axis (Fig. 2) gives a value of the uniaxial anisotropy constant. The anisotropy energy is given to first order by $E_A = K_1 \sin^2\theta$, where K_1 is the anisotropy constant, and, if K_1 is negative, θ is the angle between the magnetization and the c axis. K_1 can be calculated from $K_1 = -\frac{1}{2}MH_A$, where M is the magnetic moment per unit volume of the single-domain particle and the anisotropy field H_A is the equivalent field required to align the magnetic moment in the hard direction.

The values of K_1 of the three samples decrease as a function of the temperature (Fig. 5) because at higher temperatures the spins sample over a wider angle, so that the average effect becomes more nearly isotropic. The anisotropy energy varies more rapidly with temperature than the magnetization. In general a relation

$$K_1(T)/K_1(0) = (\sigma_{0,T}/\sigma_{0,0})^n$$

is expected if the effect of thermal expansion is neglected. Carr[23] calculated that for a hexagonal crystal structure $n = 3$. Our results are in fair agreement with this prediction. Values $n = 3.6$, $n = 3.3$, and $n = 3.1$ were found for $Fe_{1.80}Ge$, $Fe_{1.67}Ge$, and $Fe_{1.55}Ge$, respectively (Fig. 6).

B. Mössbauer measurements

Mössbauer spectra of $Fe_{1.80}Ge$, $Fe_{1.67}Ge$, and $Fe_{1.55}Ge$ were obtained with and without an external magnetic field H_{ext} applied parallel to the propagation direction of the γ rays (Figs. 7 and 8). The spectra taken with absorber C in $H_{ext} = 0$ are

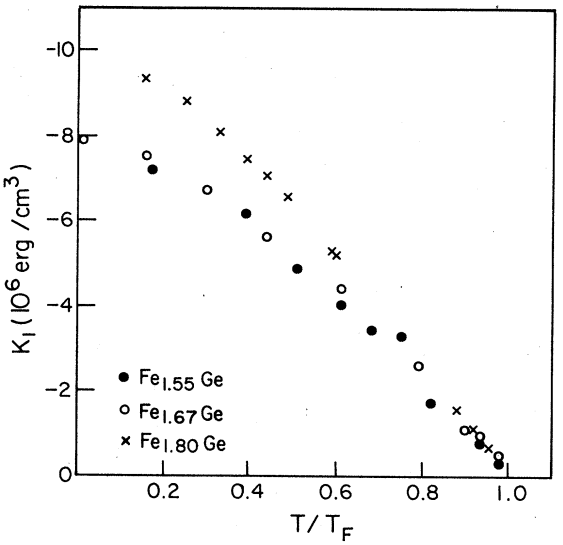

FIG. 5. Temperature dependence of the anisotropy constant K_1 for $Fe_{1.80}Ge$, $Fe_{1.67}Ge$, and $Fe_{1.55}Ge$.

similar to those found in the literature.[9,17,18] A close comparison is difficult however because the statistics obtained for the earlier spectra are not always adequate[17] and in one case[9] a different convention has been used for the velocity sign.

Clearly, the spectra consist of several overlapping absorption patterns. The outside lines of three components are well resolved for absorber B in $H_{ext} > 25$ kOe for the $Fe_{1.80}Ge$ and $Fe_{1.67}Ge$ compositions. The inside lines of these patterns are poorly or not resolved at all. For this reason it is necessary to use constraints between the linewidths and between the depth of the absorption lines of the two patterns with the smallest intensities. An attempt was made to find constraints

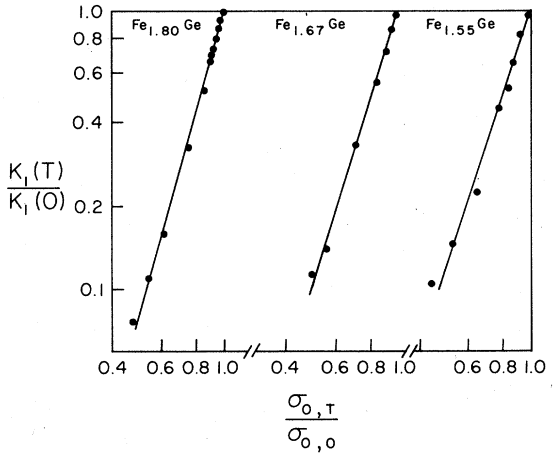

FIG. 6. $K_1(T)/K_1(0)$ plotted against $\sigma_{0,T}/\sigma_{0,0}$ on a logarithmic scale for $Fe_{1.80}Ge$, $Fe_{1.67}Ge$, and $Fe_{1.55}Ge$.

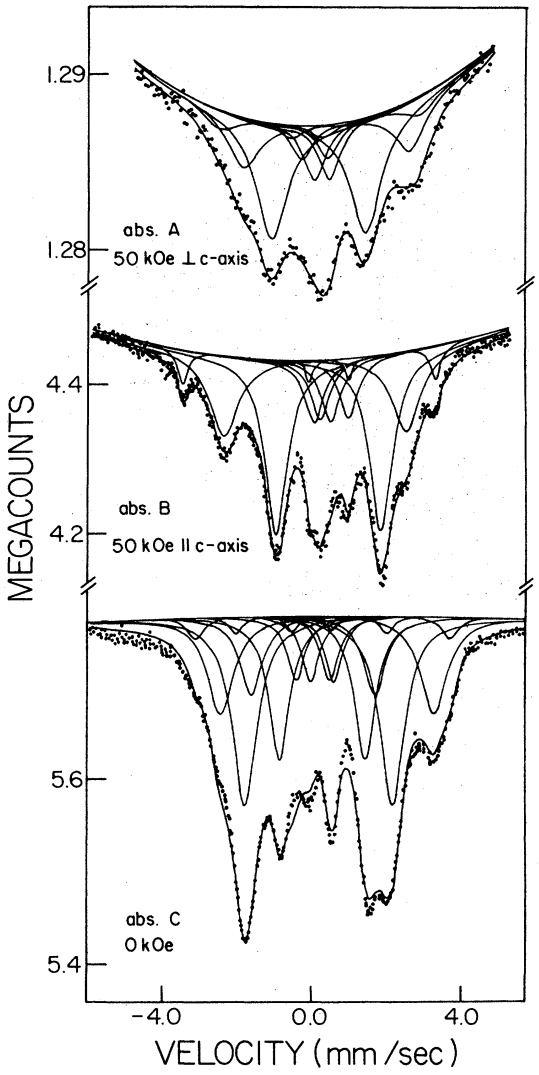

FIG. 7. Mössbauer spectra of $Fe_{1.67}Ge$ at room temperature.

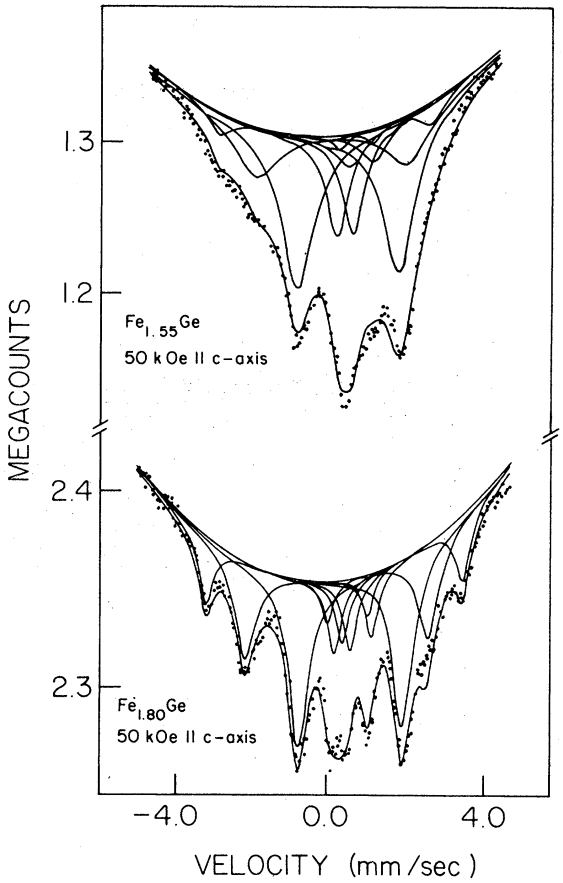

FIG. 8. Mössbauer spectra of B-type absorbers of $Fe_{1.55}Ge$ and $Fe_{1.80}Ge$.

which could be used to fit all spectra obtained for the various absorbers of different compositions. It was concluded that this procedure was possible if the linewidths and depths were assumed to decrease from the outside to the inside for each pattern according to the ratio 3:2.5:2. It should be noted that in that case the area ratios are 2.3:1.6:1. These ratios are comparable with values usually found for absorbers of this thickness.

The spectra of absorbers A and B in external fields were fitted with three absorption patterns consisting of four Lorentzians. Attempts to fit the spectra of absorber B with one or more six-line components, leaving the depths of the two and five lines as free parameters, gave negligible intensities for these lines. This finding is consistent with the presence of a collinear spin structure in these samples in an external field of 50 kOe. The results of the three component fit are shown in Table IV. The components are labeled a, d, and c. The uncertainties are indicated in brackets; they were found by comparing the results obtained for various sets of constraints. The statistical errors obtained from the fit which was finally selected as described above are substantially smaller.

The spectra above T_F (Fig. 9) do not change visibly with the iron concentration. The spectra are asymmetric but individual components are not resolved. By using the intensity ratios found for absorber B as constraints, the single-crystal spectra were fitted for various guesses for the values of the isomer shifts δ and quadrupole splittings ϵ. Only one type of fit gave acceptable results for all three compositions. The results are shown in Table V.

The Curie temperatures $T_F = 510$ K for $Fe_{1.95}Ge$ and $T_F = 490$ K for $Fe_{1.70}Ge$, and also the values obtained for the single-crystal samples (Table V) are in good agreement with those determined from magnetization measurements by Kanematsu.[8]

TABLE IV. Experimental values of the outer linewidths Γ (mm/sec), the isomer shifts δ relative to metallic iron (mm/sec), the quadrupole splitting ϵ' (mm/sec), and the hyperfine fields (kOe) for the lattice positions 2(*a*), 2(*d*), and 2(*c*) in β-phase FeGe. The relative intensities of the three components in the Mössbauer spectra are given by the ratios of A_a, A_d, and A_c. The figures in parentheses are the probable errors.

	$Fe_{1.55}Ge$		$Fe_{1.67}Ge$			$Fe_{1.80}Ge$	
	Abs. *C*	Abs. *B*	Abs. *C*	Abs. *B*	Abs. *A*	Abs. *C*	Abs. *B*
H_{ext}	0 kOe	50 kOe	0 kOe	50 kOe	50 kOe	0 kOe	50 kOe
$(A_d+A_c)/A_a$	0.59(5)	0.56(5)	0.67(5)	0.67(3)	0.60(5)	0.80(2)	0.84(2)
A_c/A_d	0.34(5)	0.25(5)	0.16(5)	0.14(4)	0.37(8)	0.63(3)	0.51(2)
Component *a*							
Γ	0.7(1)	1.1(1)	0.81(5)	0.72(5)	0.9(1)	0.55(5)	0.65(5)
δ	0.28(1)	0.34(2)	0.27(2)	0.39(1)	0.36(2)	0.32(1)	0.38(1)
ϵ'	−0.13(1)	0.14(3)	−0.098(5)	0.18(1)	−0.07(1)	−0.12(1)	0.23(1)
H_{hf}	−114(1)	−83(1)	−122(1)	−86(1)	−77(2)	−119(1)	−84(1)
Component *d*							
Γ	0.8(1)	1.4(1)	0.86(5)	0.92(5)	1.0(1)	0.55(5)	0.60(5)
δ	0.37(1)	0.34(2)	0.26(2)	0.37(1)	0.38(2)	0.34(1)	0.39(1)
ϵ'	0.41(2)	−0.85(4)	0.38(4)	−0.51(2)	0.33(1)	0.24(1)	−0.53(1)
H_{hf}	−141(2)	−124(1)	−176(1)	−150(1)	−135(3)	−174(1)	−148(1)
Component *c*							
Γ	0.7(1)	0.7(1)	0.52(5)	0.30(5)	1.0(1)	0.50(5)	0.47(5)
δ	0.32(2)	0.20(1)	0.17(2)	0.22(2)	···	0.17(1)	0.22(2)
ϵ'	0.36(5)	−0.86(2)	0.29(2)	−0.53(2)	···	0.30(1)	−0.36(1)
H_{hf}	−176(2)	−175(3)	−211(2)	−208(1)	−163(4)	−216(2)	−208(1)

The temperature dependences of H_{hf} have been determined using the enriched $Fe_{1.95}Ge$ and $Fe_{1.70}Ge$ samples. The spectra below T_F have been fitted in the same way as those obtained for the single-crystal absorbers. At temperatures above room temperature it was sometimes necessary to constrain the ratio of the linewidths of the *c* and *d* components.

IV. DISCUSSION

We will first discuss the ratios of the areas A_a, A_d, and A_c of the three absorption patterns. From the values of $(A_d+A_c)/A_a$ in Table IV it is clear that the component *a*, with the smallest H_{hf}, corresponds to iron atoms at 2(*a*) sites, if at least we assume that the distribution of atoms as proposed previously[5,7] is approximately correct. The next problem to consider is whether the two components *d* and *c* in the spectra correspond to iron atoms located at, respectively, the 2(*d*) and 2(*c*) sites[9,18] or to iron atoms at the 2(*d*) site only. This last case refers back to the model of Fatseas *et al.*[17,19] who proposed that the spectra can be fitted assuming the existence of various hyperfine fields which are due to a random distribution of vacancies in neighboring 2(*d*) shells. In this model the area A_c should correspond to iron atoms at 2(*d*) sites with no vacancies in the nearest 2(*d*) shell. For a binomial distribution the values of A_c/A_d for $Fe_{1.55}Ge$, $Fe_{1.67}Ge$, $Fe_{1.80}Ge$, and $Fe_{1.95}Ge$ are theoretically 0.03, 0.10, 0.33, and 2.8, respectively. The experimental values 0.25, 0.14, 0.51 (Table IV), and 1.1 are not in good agreement with this. In an external field the *c* and *d* components in absorber *B* behave significantly differently. It is not clear why this should be so if the only difference is the number of vacancies at a distance of 3.42 Å which is not even the nearest neighboring shell (Table VI). Finally the change in the hyperfine

TABLE V. Experimental values of the linewidths Γ, isomer shifts δ, and quadrupole splittings $\epsilon=\frac{1}{4}eQV_{zz}(1+\frac{1}{3}\eta^2)^{1/2}$ (all in mm/sec) measured at 520 K, and the values of the Curie temperatures T_F.

		2(*a*)		2(*d*)		2(*c*)		
	Γ	δ	ϵ	δ	ϵ	δ	ϵ	T_F (K)
$Fe_{1.55}Ge$	0.32(1)	0.14(1)	0.21(1)	0.13(1)	0.36(1)	0.10(2)	0.39(5)	436(1)
$Fe_{1.67}Ge$	0.33	0.13	0.21	0.13	0.37	0.11	0.39	480
$Fe_{1.80}Ge$	0.30	0.14	0.20	0.15	0.32	0.11	0.35	496

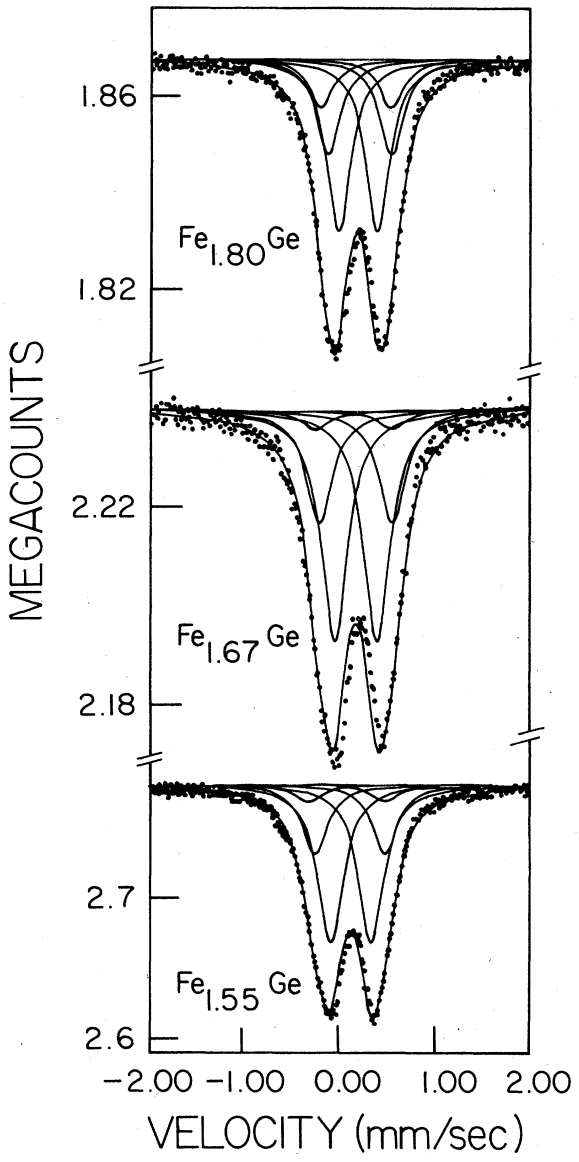

FIG. 9. Mössbauer spectra of $Fe_{1.80}Ge$, $Fe_{1.67}Ge$, and $Fe_{1.55}Ge$ at 520 K.

field per vacancy ΔH is for iron atoms at the 2(d) sites ~2 times as big as for those at 2(a) sites.[17] For the 2(a) sites the vacancies are nearer (2.64 Å) and it seems more likely that ΔH values for 2(a) and 2(d) sites should be about the same in magnitude. Indeed, from Table IV it may be seen that the linewidths of the a and α components are very similar.

In consideration of these arguments we conclude that it is more likely that the a, d, and c components correspond to iron atoms at 2(a), 2(d), and 2(c) sites. From the ratios of A_a, A_d, and A_c a good estimate of the iron distribution can be obtained. In order to obtain also an estimate of the distribution of Ge atoms and vacancies in the unit cell, the observed x-ray diffraction line intensities (Table VII) can be compared with the intensities calculated[24] from

$$jF^2(1+\cos^2 2\theta)/\sin^2\theta\cos\theta\,.$$

The distributions for which the calculated intensities fit the experimental results best (Table VII) are listed in Table VIII. The atomic distribution proposed by Kanematsu[7] is also presented in this Table. The discrepancy between the two is most significant for the $Fe_{1.80}Ge$ compound.

The results in Table VIII indicate that the 2(a) sites are almost completely occupied by iron atoms. The remaining iron atoms prefer the 2(d) sites, but when these sites are approximately half filled then the iron atoms will occupy the 2(c) site.

A study of the isomer shifts δ in Table IV shows that the differences in δ between A, B, and C type absorbers are often larger than the errors quoted. This discrepancy can partially be related to the difficulties in fitting the unresolved inside absorption lines.

The isomer-shift values δ do not change significantly with the iron concentration (Tables IV and V). The values of δ are consistently smaller for the 2(c) site than those for the other two sites which are approximately equal. It follows that either the occupation of 3d orbitals is smaller or

TABLE VI. Neighbors of the 2(a), 2(d), and 2(c) sites.

2(a)	2(d)	2(c)
2 2(a) sites at 2.51 Å	3 2(c) sites at 2.32 Å	3 2(d) sites at 2.32 Å
6 2(d) sites at 2.64 Å	2 2(c) sites at 2.51 Å	2 2(d) sites at 2.51 Å
6 2(c) sites at 2.64 Å	6 2(a) sites at 2.64 Å	6 2(a) sites at 2.64 Å
6 2(a) sites at 4.01 Å	6 2(d) sites at 3.42 Å	6 2(c) sites at 3.42 Å
	6 2(a) sites at 4.01 Å	6 2(a) sites at 4.01 Å
	6 2(d) sites at 4.01 Å	6 2(c) sites at 4.01 Å

TABLE VII. Experimentally observed values of the relative x-ray diffraction intensities are compared with values calculated from atomic distributions proposed (a) in this work, and (b) in Ref. 8.

	$Fe_{1.55}Ge$			$Fe_{1.67}Ge$			$Fe_{1.80}Ge$		
$(hk \cdot l)$	Obs.	Calc.[a]	Calc.[b]	Obs.	Calc.[a]	Calc.[b]	Obs.	Calc.[a]	Calc.[b]
(10.1)	31	29	23	20	19	18	16	12	11
(00.2)	5	5	6	10	7	7	7	8	8
(10.2)	98	97	96	96	95	95	97	93	93
(11.0)	100	100	100	100	100	100	100	100	100
(20.1)	5	6	5	3	4	4	2	2	2
(11.2)	7	8	9	10	10	10	10	11	11
(10.3)	5	4	3	4	3	3	2	2	2
(20.0)	24	28	28	26	28	28	30	27	27

[a] This work.
[b] Ref. 8.

the occupation of 4s orbitals is larger for iron atoms at 2(c) sites compared to those at 2(d) and 2(a) sites. Since the hyperfine fields H_{hf} for the 2(c) sites are larger than for the other two sites the first possibility is more likely.

Above T_F the quadrupole splitting is given by $\epsilon = \frac{1}{4}eQV_{zz}(1+\frac{1}{3}\eta^2)^{1/2}$. The experimental values of ϵ (Table V) and H_{hf} (Table IV) show that the energy shift due to the electric quadrupole interaction is much less than that due to the magnetic dipole interaction: $eQV_{zz} \ll \mu H_{hf}$. By using first-order perturbation theory a nuclear state with spin $I = \frac{3}{2}$, subjected to a magnetic field H_{hf} and an electric field gradient (EFG) defined by V_{zz} and $\eta = (V_{xx} - V_{yy})/V_{zz}$ has energy eigenvalues given by

$$E = -g\mu_N H_{hf} m_I + (-1)^{|m_I|+1/2}\tfrac{1}{4}eQV_{zz}f(\theta,\phi) \quad (1)$$

TABLE VIII. Average number of Fe and Ge atoms per unit cell on the 2(a), 2(d), and 2(c) sites. Under (a) the distribution previously proposed (Ref. 7) are given.

	(a)					
	2(a)		2(d)		2(c)	
Composition	Fe	Ge	Fe	Ge	Fe	Ge
$Fe_{1.80}Ge$	1.86	0.00	0.99	0.36	0.50	1.50
$Fe_{1.67}Ge$	1.95	0.00	1.16	0.10	0.15	1.85
$Fe_{1.55}Ge$	1.95	0.00	0.86	0.16	0.21	1.79
	(b)					
	2(a)		2(d)		2(c)	
Composition	Fe	Ge	Fe	Ge	Fe	Ge
$Fe_{1.80}Ge$	2.00	0.00	1.55	0.00	0.02	1.98
$Fe_{1.67}Ge$	2.00	0.00	1.34	0.00	0.00	2.00
$Fe_{1.55}Ge$	2.00	0.00	1.16	0.04	0.00	2.00

with

$$f(\theta,\phi) = \tfrac{3}{2}\cos^2\theta - \tfrac{1}{2} + \tfrac{1}{2}\eta\sin^2\theta\cos 2\phi\,, \quad (2)$$

where θ and ϕ are the conventional spherical polar angles of the magnetic field with respect to the (x,y,z) frame which diagonalizes the EFG tensor. In addition to a nonspherically symmetric EFG the hyperfine field can also be anisotropic in the sense that its magnitude changes with orientation. If the anisotropic part H_{an} is much smaller than the isotropic part, the hyperfine field can in first-order perturbation be written as

$$H_{hf} = H_{is} + H_{an} = H_{is} + D_{an}f(\theta,\phi)\,, \quad (3)$$

where $f(\theta,\phi)$ is given by (2) and η is the asymmetry parameter of the hyperfine field tensor. For our samples we assume that both the EFG and hyperfine field tensor are diagonalized by choosing the z axis along the uniaxial c axis and the x and y axes in the basal plane of the unit cell.

The shift of the nuclear Zeeman levels due to an EFG or an anisotropic hyperfine field at the nucleus depends in both cases on the angular function $f(\theta,\phi)$. This function can be considered for two particular geometries which will be of interest for the interpretation of the results obtained for absorbers A, B, and C.

If $\theta = 0$, then $f(\theta,\phi) = 1$, independent of θ and η. This arrangement corresponds to the magnetization lying along the z direction assumed to be the c axis. This situation is encountered for absorber B in external fields $H_{ext} > 25$ kOe. If $\theta = 90°$, then $f(\theta,\phi) = -\frac{1}{2} + \frac{1}{2}\eta\cos 2\phi$. The value depends upon η and ϕ, corresponding to the magnetization being in the basal plane, as for absorbers A and C. The average value of the function is $f(\theta,\phi) = -\frac{1}{2}$ with a standard deviation of $\eta/\sqrt{8}$.

So from Eq. (1) the quadrupole shift changes from $-\frac{1}{8}eQV_{zz}$ to $\frac{1}{4}eQV_{zz}$. This behavior is reasonably well confirmed by the experimental values of ϵ' in Table IV. Here ϵ' is obtained from $\epsilon' = \frac{1}{2}(\Delta_{56} - \Delta_{12})$, where Δ_{ij} is the difference in the positions of the absorption lines i and j. Comparing the results for absorbers C and B, ϵ' changes sign and its absolute value is increased approximately by a factor of 2 for all three components. These results are therefore in fair agreement with our assumptions regarding the directions of the principle axis of the EFG tensor. The quadrupole shift $\frac{1}{4}eQV_{zz}$ can now be calculated for the 2(a), 2(d), and 2(c) sites from the values of ϵ' for absorbers B and C.

Systematic errors in the values of ϵ' are probably related to difficulties in fitting the unresolved inside absorption lines. The differences in δ between absorbers B and C indicate that such errors exist. The quadrupole shifts can also be calculated for each component from the difference in the center of the resolved outside lines in the spectra for absorbers B and C. This difference should be equal to $\frac{3}{8}eQV_{zz}$. The values of $\frac{1}{4}eQV_{zz}$ calculated in these two ways have been averaged and are shown in Table IX.

The quadrupole shifts obtained for the three sites are temperature independent. Figure 10 shows the results found for $Fe_{1.70}Ge$. The values for the 2(d) and 2(c) sites are close to those above T_F. For the 2(a) sites the value above T_F is ~2 times the value below T_F. This difference could indicate that the asymmetry parameter for this site is substantial. In addition the average V_{zz} direction can deviate from the c-axis direction as a result of the vacancies in the nearest-neighbor shell.

The values of the Γ shown in Table IV show that the absorption lines are considerably broadened. Line broadening can result from the random distribution of vacancies over the 2(d) sites, since H_{hf}, δ, and the EFG tensor may depend on the number of vacancies in neighboring shells of an iron atom. A distribution in H_{hf} values is probably mainly responsible for the broadening because the narrow linewidths of the spectra at 520 K indicate that δ and $\frac{1}{4}eQV_{zz}(1+\frac{1}{3}\eta^2)^{1/2}$ are not much affected by the vacancy distribution.

TABLE IX. Average values of $\frac{1}{4}eQV_{zz}$ in mm/sec at room temperature for the 2(a), 2(d), and 2(c) sites.

	$Fe_{1.55}Ge$	$Fe_{1.67}Ge$	$Fe_{1.80}Ge$
2(a)	0.11(2)	0.11(2)	0.14(2)
2(d)	−0.42(1)	−0.34(5)	−0.24(3)
2(c)	−0.43(5)	−0.27(3)	−0.23(6)

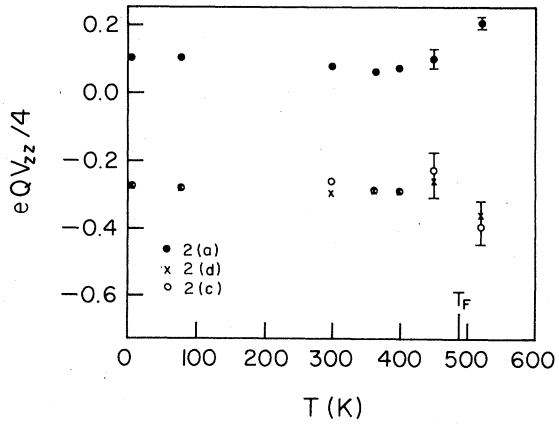

FIG. 10. $\frac{1}{4}eQV_{zz}$ as a function of the temperature T for $Fe_{1.70}Ge$.

The values of the magnetic hyperfine fields $H_{hf}(T)$ are represented in Table X. For the 2(d) and 2(c) sites the values of $H_{hf}(0)$ are slightly larger for $Fe_{1.70}Ge$ compared with those for $Fe_{1.95}Ge$. The hyperfine field $H_{hf}(0)$ at an Fe^{57} nucleus can be thought of as arising from a core polarization and a conduction-electron polarization contribution: $H_{hf}(0) = H_{cp} + H_{ce}$. The last part can be split up in a term due to the polarization of the conduction electrons by the atom itself and another due to the sum of polarization effects produced by all neighbors: $H_{ce} = H_s + H_\Sigma$. The value of H_Σ for a central iron atom depends on the number of iron atoms in neighboring shells and the distance of these shells from the iron atom.

Therefore, the line broadening in the three absorption patterns is thought to be mainly due to the random distribution of iron atoms in the 2(d) and 2(c) shells, which will result in a distribution of H_Σ values. Also the difference in the average values of the hyperfine fields found at the three lattice sites could partially be explained by different average values of H_Σ for these sites. The neighbors of the three sites are shown in Table VI. The average iron concentration in each neighbor shell can be calculated from Table IV. Thus it is clear that the average distribution of iron atoms around the 2(a), 2(d), and 2(c) sites are different. However, it is difficult to estimate the value of H_Σ for each site, because the polarization effects of iron atoms in the subsequent shells are not known. A good estimate of the influence of the iron concentration in neighboring shells on the average values of $H_{hf}(0)$ can be obtained by comparing the hyperfine fields measured for $Fe_{1.95}Ge$ and $Fe_{1.70}Ge$. If H_Σ is assumed to make a negative contribution to $H_{hf}(0)$, then the average values of $|H_{hf}(0)|$ for the three sites are expected to increase with increasing iron concentration in neighboring shells. Therefore the

TABLE X. Experimental values of the magnetic hyperfine fields (kOe) and the average outer linewidths (mm/sec) for the lattice sites 2(*a*), 2(*d*), and 2(*c*) as a function of temperature.

	$Fe_{1.70}Ge$					$Fe_{1.95}Ge$			
T (K)	2(*a*)	2(*d*)	2(*c*)	$\bar{\Gamma}$	*T* (K)	2(*a*)	2(*d*)	2(*c*)	$\bar{\Gamma}$
4.2	142(1)	215(1)	265(2)	0.77	4.2	140(1)	204(1)	254(1)	0.81
78	139	211	261	0.80	78	138	202	245	0.70
300	118	172	218	0.84	300	121	175	218	0.88
364	106	153	196	0.77	410	94	134	163	0.70
401	95	136	173	0.75	480	61	82	104	0.85
452	71	99	124	0.72					

values of $|H_{hf}(0)|$ should be larger for $Fe_{1.95}Ge$ than for $Fe_{1.70}Ge$ if H_L plays a dominant role in determining the magnitude of average hyperfine fields. This feature is not observed. For the 2(*d*) and 2(*c*) sites even a slight decrease in the values of $H_{hf}(0)$ is found for $Fe_{1.95}Ge$ compared to those of $Fe_{1.70}Ge$. It can be concluded therefore that either the change in the average value of H_L is compensated by changes in H_{cp} and H_s, or that the average values of $H_{hf}(0)$ for the 2(*a*), 2(*d*), and 2(*c*) sites are mainly determined by the values of H_{cp} and H_s which are both proportional to the magnetic moment of the iron atom. Then the ratio of the $H_{hf}(0)$ values for the 2(*a*), 2(*d*), and 2(*c*) sites is in good approximation equal to the ratio of magnetic moments at these sites. From Table X the ratio of the hyperfine fields averaged for the two samples is 1:1.48:1.84 for the 2(*a*), 2(*d*), and 2(*c*) sites. This result can be used for the interpretation of the magnetization data. For a collinear spin structure the magnetic moments per formula unit (Table III) are given by $n_a\mu_a + n_d\mu_d + n_c\mu_c$. By using the concentrations n_a, n_d, and n_c of iron atoms on 2(*a*), 2(*d*), and 2(*c*) sites from Table IV, the iron magnetic moments $\mu_a = 1.30(5)\mu_B$, $\mu_d = 1.93(7)\mu_B$, and $\mu_c = 2.4(1)\mu_B$ are found. The value of the magnetic moment at the 2(*a*) site is in excellent agreement with those determined from neutron diffraction measurements[5,6,11] (Table I). There is no agreement in the literature about the value of μ_d however. The present value of μ_d is the same as that reported by Forsyth and Brown[6] from measurements on single-crystal $Fe_{1.67}Ge$. No value for μ_c was reported which is not surprising since the concentration of iron atoms at 2(*c*) sites is very small for this composition.

In order to obtain information about the character of the exchange interactions in these samples, it is useful to study the behavior of $H_{hf}(T)/H_{hf}(0)$ and $\sigma_{0,T}/\sigma_{0,0}$ against T/T_F. If short-range nearest-neighbor exchange interactions are mainly responsible for the ferromagnetic ordering then the iron concentration in neighboring shells should affect the temperature dependence of the reduced hyperfine field at a particular site. Then the temperature dependence of $H_{hf}(T)/H_{hf}(0)$ for the 2(*a*), 2(*d*), and 2(*c*) sites could be different. Furthermore, since the concentration of iron atoms in the 2(*d*) and 2(*c*) shells is smaller for the low-iron-concentration region $H_{hf}(T)/H_{hf}(0)$ and $\sigma_{0,T}/\sigma_{0,0}$ are expected to decrease faster with increasing T/T_F

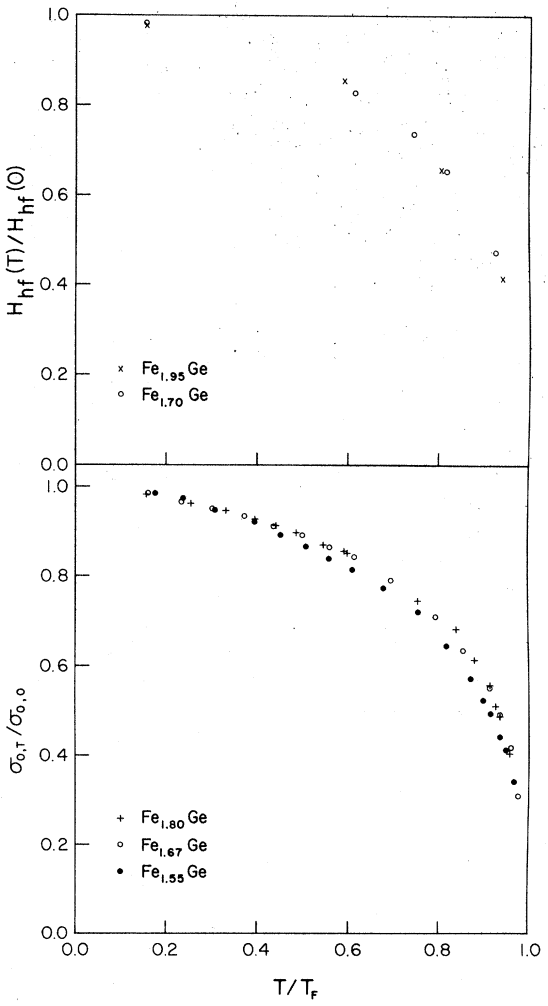

FIG. 11. Average hyperfine field and the magnetization as a function of temperature.

than for the high-iron-concentration region. Finally as a result of the random distribution of iron atoms in 2(d) and 2(c) shells the line broadening of the Mössbauer lines should be affected by a change in temperature if short-range exchange interactions are responsible for the magnetic order.

In Fig. 11 the values of $\sigma_{0,T}/\sigma_{0,0}$ and those of $H_{hf}(T)/H_{hf}(0)$ averaged for the three components are plotted against T/T_F. For $Fe_{1.55}Ge$ $\sigma_{0,T}$ decreases faster with temperature than for the $Fe_{1.67}Ge$ and $Fe_{1.80}Ge$. It is not certain whether this behavior is caused by short-range interactions since $\sigma_{0,T}$ for $Fe_{1.80}Ge$ and $Fe_{1.67}Ge$ and also $H_{hf}(T)$ for $Fe_{1.95}Ge$ and $Fe_{1.70}Ge$ have the same temperature dependence. Since the rate of decrease in T_F with iron concentration is much lower between $Fe_{1.95}Ge$ and $Fe_{1.67}Ge$ than between $Fe_{1.67}Ge$ and $Fe_{1.55}Ge$ it is possible that the character of the exchange interaction has changed.

A study of the $H_{hf}(T)$ and $\bar{\Gamma}(T)$ values presented in Table X however indicates that weak iron-iron nearest-neighbor exchange interactions are present. The hyperfine field values decrease slightly faster with temperature for the 2(d) and 2(c) sites than for the 2(a) site. In addition the change in linewidth between 4.2 K and T_F is insignificant. If no short-range exchange interaction was present, then Γ should decrease with increasing temperature. The decrease should be proportional to the decrease in the average field since the linewidth broadening primarily has its origin in the distribution of H_{hf}.

It can be concluded therefore that the exchange interaction mainly responsible for magnetic order is of a long-range nature. Short-range exchange interactions are present but are relatively weak.

An analysis of the H_{hf} values measured for absorbers A, B, and C gives information about the spin structure in the β-phase region and about the anisotropy contribution to the hyperfine field at room temperature. The results of a more extensive study of $Fe_{1.67}Ge$, using a greater variety of external fields have been discussed before.[10] The present H_{hf} values obtained for $Fe_{1.67}Ge$ are the results of a new measurement (abs C) or new fits (abs B and A), using a fitting method slightly different from that of Ref. 10. The new results are essentially the same as those presented before. The H_{hf} values measured for $Fe_{1.80}Ge$ for absorbers B and C are in good agreement with those of the $Fe_{1.67}Ge$ sample whereas those of $Fe_{1.55}Ge$ are slightly smaller. It should be noted however that the T_F value of this last composition is substantially less (~50 K) than those of $Fe_{1.67}Ge$ and $Fe_{1.80}Ge$ (Table V).

For disk-shaped absorbers consisting of ferromagnetic powder particles of arbitrary shapes, the field H_{int} acting on the iron magnetic moments is not well known. For a spherical particle H_{int} can be described by[25] $H_{int}=H_{ext}-H_D+H_L$, where $H_D=4\pi\delta M+\frac{4}{3}\pi M$ and $H_L=\frac{4}{3}\pi\delta M$. Here δ is the volume fraction occupied by the magnetic material. By using $\delta=\frac{1}{3}$ and the results of the magnetic measurements, a value $H_D-H_L=5$ kOe is found.

For a collinear spin structure with a completely isotropic magnetic hyperfine field, the value of H_{hf} in the presence of an external field is given by $H_{hf}(H_{ext})-H_{int}=H_{hf}(0)$. This relation is reasonably satisfied, for absorber A (Table IV, Ref. 10) but not for absorber B. It follows that the hyperfine fields at the iron nuclei are anisotropic. From Eq. (3) the difference between the values of $H_{hf}(0)$, measured for absorber C, and $H_{hf}(H_{ext})-H_{int}$ found for absorber B is given by

$$\tfrac{3}{2}D_{an}=[H_{hf}(H_{ext})-H_{int}]-H_{hf}(0).$$

The values for D_{an} calculated from this relation for iron atoms at 2(a), 2(d), and 2(c) sites do not change significantly with iron concentration (Table XI). D_{an} has the largest value for iron atoms at the 2(c) site. The anisotropic hyperfine field can be partially ascribed to the dipolar field caused by the surrounding dipoles. This contribution depends on the iron-atom distribution in neighboring shells. From the lattice sum using $\mu_a=1.3$, $\mu_d=1.9$, and $\mu_c=2.4\mu_B$, we find contributions to D_{an} of −1(1) kOe, 2(1) kOe, and 2(1) kOe, for 2(a), 2(d), and 2(c) sites, respectively. The uncertainties in brackets reflect the influence of different iron dis-

TABLE XI. Values of the anisotropic hyperfine field component D_{an} (kOe) uncorrected (a) and corrected (b) for the demagnetization and Lorentz fields. H_{dip}^{calc} is the total dipolar field which has been calculated as explained in the text.

	$Fe_{1.55}Ge$		$Fe_{1.67}Ge$		$Fe_{1.80}Ge$		
Site	(a)	(b)	(a)	(b)	(a)	(b)	H_{dip}^{calc}
2(a)	−13(1)	−9(2)	−10(1)	−6(2)	−10(1)	−7(2)	+7(2)
2(d)	−22(3)	−19(3)	−17(1)	−13(2)	−16(1)	−13(2)	−18(5)
2(c)	−33(3)	−29(4)	−32(2)	−28(3)	−28(2)	−25(3)	−15(2)

tributions on the values of the dipolar fields.

The second contribution to D_{an} arises from the spin moment of the $3d$ electrons of the iron atom itself. Since the charge and spin asymmetries are both due to holes in the $3d$ shell, the EFG and dipolar field can be assumed to be proportional to each other,[26] neglecting spin-polarization effects.[27] Then the dipolar fields due to an asymmetric spin distribution at the iron atoms can be estimated from $H_{dip} = \mu_B V_{zz}$. V_{zz} can be calculated from the average values of $\frac{1}{4}eQV_{zz}$ from Table IX, taking $Q = 0.2$ b for the ^{57}Fe nucleus. Shielding effects ($R = 0.1$ for an Fe^{2+} ion[28]) and also the lattice term in V_{zz} are neglected. Values for H_{dip} of 8(1), −20(4), and −17(1) kOe are found for the iron atoms at 2(a), 2(d), and 2(c), respectively. Adding to this the contributions from the lattice we obtain the total dipolar-field contributions H_{dip}^{calc} (Table XI) to D_{an}. The values obtained for the 2(d) and 2(c) sites are in reasonable agreement with the experimental values, considering the assumptions made in the calculation. However, the agreement is probably fortuitous since the value of H_{dip}^{calc} for the 2(a) site has the wrong sign. Another orientation-dependent term which should be considered is the field at the ^{57}Fe nucleus from an unquenched orbital angular momentum. This field is proportional to $g-2$. No data about the anisotropy in g are available yet at room temperature.

It is interesting to compare the D_{an} values in Table XI with the anisotropy constants K_1 shown in Fig. 5. The K_1 values for $Fe_{1.67}Ge$ and $Fe_{1.55}Ge$ are the same, whereas K_1 for the $Fe_{1.80}Ge$ sample is much higher at low temperatures. If the origin of the magnetic anisotropy is in the single-ion anisotropy of the iron atoms, this observation can be correlated with the concentration of iron atoms at the 2(c) sites. As shown in Table VIII, for $Fe_{1.80}Ge$ this concentration is much higher than for the $Fe_{1.55}Ge$ and $Fe_{1.67}Ge$ samples. Hence the single-ion anisotropy of iron atoms at 2(c) sites appears to be larger than that at the other two sites. Mössbauer-effect measurements have also shown that for the 2(c) sites the anisotropic contribution to H_{hf} is largest.

For external fields larger than 20 kOe the $Fe_{1.67}Ge$ spectra can be fitted with three four-line-absorption patterns. Also, for absorber A the relation $H_{hf}(H_{ext}) - H_{int} = H_{hf}(0)$ is satisfied within the errors of measurement. It can be concluded that for $H_{ext} \geq 20$ kOe the canting of the spins is zero in $Fe_{1.67}Ge$ or at most small. We will assume that this is also true for other alloys in the β-phase region.

By combining the results of the Mössbauer and magnetization measurements it is possible to obtain information about the spin structure for $H_{int} = 0$. The magnetic moment per formula unit in the presence of canting angles θ for $H_{int} = 0$ is given by

$$m(\theta) = n_a\mu_a\cos\theta_a + n_d\mu_d\cos\theta_d + n_c\mu_c\cos\theta_c . \quad (4)$$

The iron concentrations n_a, n_d, and n_c at the three lattice sites can be obtained from Table VIII. $m(\theta)$ can then be calculated as a function of θ by using the magnetic moment proposed in the present work or those shown in Table I. Because the canting angles are decreasing, $m(\theta)$ is expected to increase with increasing external field. The canting has become zero for $H_{ext} = 20$ kOe. Experimentally an increase of 3(1)% is found for all three samples when H_{ext} is increased to this value. At least part of this change is due to the high-field susceptibility of the material. Consequently the magnetization increase from the disappearance of canting must be considerably less than 3(1)%. It is clear that such a small increase in the magnetization limits the maximum values of the canting angles, if they exist for $H_{int} = 0$, considerably. As can be calculated from (4), for canting angles of 15° on the 2(a), 2(d), or 2(c) sites an increase in the magnetization of 1.5%, 1.2%, and 0.8% are expected, respectively, for $Fe_{1.80}Ge$ when the external field is increased to 20 kOe. For the magnetic moments and canting angles presented in Table I, the expected increases are substantially larger than found experimentally. For $\theta_d = 28°$ (Ref. 5) an increase of 5% is expected. In the spin structure proposed by Kanematsu and Ohoyama[7] part of the 2(a) sites have zero canting and the rest have a canting close to 90°. From this model a 50% increase in the magnetization is expected. The spin structure of Daniels *et al.*[9] with $\theta_d \approx 15°$ and $\theta_c \approx 90°$ are based on the analysis of Mössbauer spectra obtained in fields of 13.5 kOe. Then, an increase of 28% is expected from an increase of H_{ext} from 13.5 to 20 kOe. Experimentally an increase of only 1% has been found.

In conclusion, the canting angles proposed previously are too large. On the other hand, our experimental results are consistent with a collinear spin structure.

V. CONCLUSION

A study of different heat treatments shows that compositions in the high-iron-concentration region of β-phase iron germanium can be obtained pure by quenching the samples with speeds as large as possible.

The iron atoms are present at all three lattice sites. The anisotropic contributions to H_{hf} are different for the sites and as a result the three hyperfine field patterns in the Mössbauer spectrum

are resolved if an external field is applied parallel to the c axis of the hexagonal unit cell. It is then possible to measure the distribution of iron atoms fairly accurately. The results indicate that the $2(a)$ sites are almost completely occupied by iron atoms. The remaining iron atoms prefer the $2(d)$ sites, but when these sites are approximately half filled then the iron atoms will occupy the $2(c)$ sites.

The hyperfine fields are almost independent of the concentration of iron atoms in neighboring shells. Thus, it appears that the exchange interactions are of a long-range nature and that the different H_{hf} values are related to different magnetic moments at the three sites. These results, when used in the analysis of the magnetization data, yield the magnetic moments $\mu_a = 1.3$, $\mu_d = 1.9$, and $\mu_c = 2.4\mu_B$.

The anisotropy constant K_1 appears to be largest for iron atoms at the $2(c)$ sites. Also the anisotropy contribution D_{an} to H_{hf} is largest for this site. A relation $K_1(T)/K_1(0) = (\sigma_{0,T}/\sigma_{0,0})^n$ has been found, where n is between 3 and 4.

ACKNOWLEDGMENT

This research was financially supported by the National Research Council of Canada.

*Present address: Dept. of Physics and Oceanography, Royal Roads Military College, FMO Victoria, BC, Canada VOS 1B0.

[1]K. Kanematsu and T. Ohoyama, J. Phys. Soc. Jpn. 20, 236 (1965).
[2]M. Castelliz, Min. Chem. Eng. Rev. 84, 765 (1953).
[3]F. Laves and H. J. Wallbaum, Z. Angew. Min. 4, 17 (1941-2).
[4]K. Yasukochi, K. Kanematsu, and T. Ohoyama, J. Phys. Soc. Jpn. 16, 429 (1965).
[5]E. Adelson and A. E. Austin, J. Phys. Chem. Solids 26, 1795 (1965).
[6]J. B. Forsyth and P. J. Brown, in *Proceedings of the International Conference of Magnetism, Nottingham, 1964* (Institute of Physics and the Physical Society, London, 1964), p. 524.
[7]K. Kanematsu and T. Ohoyama, in Ref. 6, p. 512.
[8]K. Kanematsu, J. Phys. Soc. Jpn. 20, 36 (1965).
[9]J. M. Daniels, F. E. Moore, and S. K. Panda, Can. J. Phys. 53, 2482 (1975).
[10]N. J. G. Hall, P. J. Schurer, and A. H. Morrish, Physica B 86–88, 395 (1977).
[11]H. Katsuraki, J. Phys. Soc. Jpn. 19, 863 (1964).
[12]Y. Tawara, J. Phys. Soc. Jpn. 19, 776 (1964).
[13]J. J. Becker and E. M. Symes, J. Appl. Phys. 36, 1000 (1965).
[14]H. Yamamoto, J. Phys. Soc. Jpn. 20, 2166 (1965).
[15]G. A. Fatseas and P. Lecocq, C. R. Acad. Sci. B 262, 107 (1966).
[16]E. Germagnoli, C. Lamborizio, S. Mora, and I. Ortalli, Nuovo Cimento B 42, 314 (1966).
[17]G. A. Fatseas, J. L. Dormann, and L. Rossard, J. Phys. (Paris) 32, 785 (1971).
[18]S. C. Bhargava and P. K. Iyengar, Phys. Status Solidi. A 38, 601 (1976).
[19]G. A. Fatseas, Can. J. Phys. 54, 1850 (1976).
[20]D. Eliezer, S. Nadir, and M. Ron, J. Phys. (Paris) Colloq. 35, C61–477 (1974).
[21]T. E. Cranshaw, J. Phys. E 7, 497 (1974).
[22]J. Crangle and G. M. Goodman, Proc. R. Soc. A 321, 477 (1971).
[23]J. W. Carr, Phys. Rev. 109, 1971 (1958).
[24]N. F. M. Henry, H. Lipson, and W. A. Wooster, *The Interpretation of X-Ray Diffraction Photographs* (Macmillan, London, 1961).
[25]H. Zijlstra, *Experimental Methods in Magnetism*, (North-Holland, Amsterdam, 1967), Vol. 2, p. 82.
[26]G. J. Perlow, C. E. Johnson, and W. Marshall, Phys. Rev. 140, A875 (1965).
[27]A. J. Freeman and R. E. Watson, Phys. Rev. 131, 2566 (1963).
[28]R. M. Sternheimer, Phys. Rev. A 6, 1702 (1972).